applied optics

Bulk, cascaded pulse compression scheme and its application to spin emitter characterization

Anne-Laure Calendron,[1,2,3,*] Joachim Meier,[4] Elias Kueny,[1,2] Sven Velten,[1] Lars Bocklage,[1,3] Ralf Röhlsberger,[1,3,5] and Franz X. Kärtner[1,2,3,6]

[1]Deutsches Elektronen-Synchrotron (DESY), Notkestraße 85, 22607 Hamburg, Germany
[2]Center for Free-Electron Laser Science (CFEL), Notkestraße 85, 22607 Hamburg, Germany
[3]The Hamburg Centre for Ultrafast Imaging, Luruper Chaussee 149, 22761 Hamburg, Germany
[4]The European XFEL, Holzkoppel 4, 22869 Schenefeld, Germany
[5]Helmholtz Institut Jena and Friedrich-Schiller Universität Jena, Fröbelstieg 3, 07743 Jena, Germany
[6]Physics Department, University of Hamburg, Luruper Chaussee 149, 22761 Hamburg, Germany
*Corresponding author: anne-laure.calendron@desy.de

Received 10 November 2020; revised 28 December 2020; accepted 29 December 2020; posted 5 January 2021 (Doc. ID 412177); published 25 January 2021

The 35-fs-long pulses of a commercial Ti:sapphire amplifier are compressed to ∼20 fs via self-phase modulation in bulk glass substrates. The cascading of both nonlinear broadening and dispersion compensation stages makes use of the increasing peak power in the successive nonlinear stages. As an application example, the compressed pulses are used for electro-optical sampling of terahertz waves created by optically pumped thin-film spin emitters.

https://doi.org/10.1364/AO.412177

1. INTRODUCTION

Ultrafast laser systems with mJ-level pulse energy are widely used and commercially available. Employing Ti:sapphire as gain material, they typically deliver pulses longer than 30 fs. Many applications though require shorter pulse duration or larger spectral width. Electro-optical sampling (EOS) is one such application; it results in a convolution between the probe pulse and the waveform to sample. Pulses as short as possible are desired to reduce this averaging effect and acquire data accurately. One such example is the sampling of terahertz (THz) waveforms of sub-picosecond duration: a single cycle of 3 THz or 10 THz frequency lasts 333 fs or 100 fs, respectively.

Pulse compression was demonstrated first in 1970 by Alfano and Shapiro [1]. Spectral broadening can be achieved with self-phase modulation (SPM) alone [1], or with increased peak power inducing filamentation and the formation of a white-light continuum [2]. During nonlinear broadening, the spectrum of the pulses is widened, and the dispersion of the material stretches the pulses in time. As a result, the peak power decreases during this process. Typically, the pulses are re-compressed in time close to their Fourier transform limit after the nonlinear broadening stage. Cascading nonlinear processes and dispersion compensation stages mitigate this increase in pulse duration, making the scheme more efficient, especially when already short pulses are supposed to be further compressed. With the cascaded nonlinear processes as used in Ref. [3], 2 mJ, 1.2-ps-long pulses have been compressed to 13 fs, whereas Ref. [4] cascades broadening in bulk after a first stage in gas, extending the spectrum of the 25 fs compressed laser pulses to 500–2400 nm. A slightly different technique is presented in the work of Beetar *et al*. [5], where two stages of multi-plate compression, each followed by dispersion compensation, allowed us to reduce the 280 fs initial pulse duration down to 50 fs. There, the position of each multi-plate is optimized along the propagation direction to maximize the spectral broadening, without making use of the maximal potential peak power. Other techniques have proven to be able to shorten pulses, but at the expense of the experimental complexity. For example, with hollow-core fiber compressors [6], single to few-cycle pulses at the mJ level have been generated, and recently pulses have been reduced from 1 ps down to 66 fs [7] or from 240 fs to sub-two-cycle pulses [8]. In this scheme, other processes such as plasma defocusing, Raman shift, and self-steepening play a role. The formation of self-defocusing temporal solitons via phase-mismatched cascaded second-harmonic generation has been numerically investigated in Ref. [9].

In this paper, we report on the implementation of a simple and compact pulse compression setup, based on successive spectral broadening and dispersion compensation stages. After the description of the experimental setup, we present the results obtained with two different broadening materials. The setup is optimized once for shortest pulse duration and once for daily reproducibility. The dispersion management is discussed throughout the text. We conclude by describing the application of these shortened pulses.

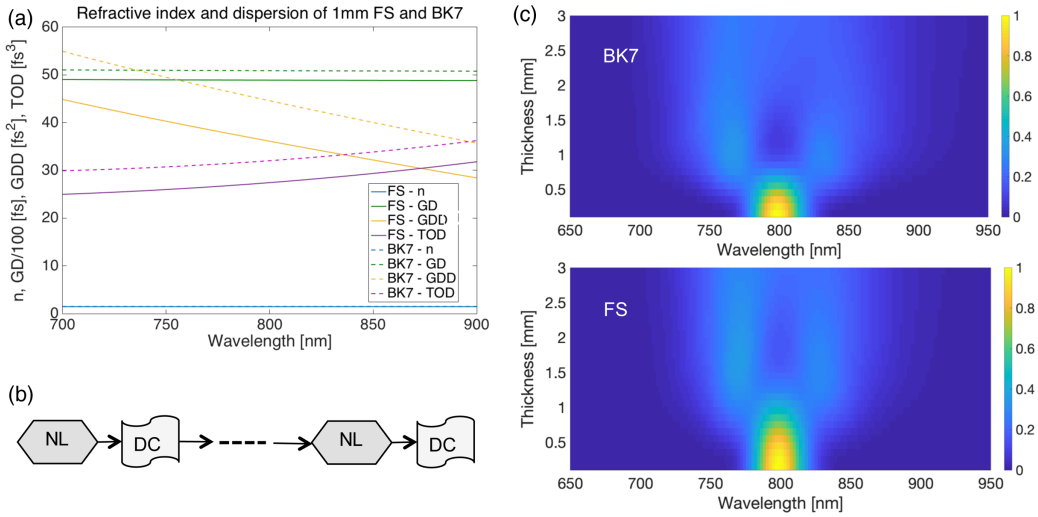

Fig. 1. (Color available online) (a) Dispersion curves of FS and BK7, per mm. (b) Schematic of cascaded setup: nonlinear broadening (NL) alternates with dispersion compensation (DC). (c) Simulations of spectral broadening: here for three passes through FS and BK7 plates with dispersion compensation, versus variations of material thickness.

2. MATERIAL AND DISPERSION MANAGEMENT

The cascading of nonlinear broadening and dispersion compensation stages makes use of the successively higher peak powers in the individual broadening stages. Several effects, which we address below, play a significant role in the compression result; among other effects count nonlinear spectral broadening, dispersion management, and/or spatial pulse breakdown (modulation instability and filamentation). In order to maintain a usable spatial profile, the latter should be avoided.

Our setup is designed to compress near-infrared (NIR) pulses in the order of 100 μJ level. The broadening step relies mainly on SPM. As the beam will be transmitted through the broadening material in each step, it needs to have a good transmission. In addition, materials with a relatively low nonlinear refractive index and high damage threshold advantageously support relatively small beam diameters, thus mitigating the risk of beam breakup and avoiding white-light generation. We chose fused silica (FS) and borosilicate glass (BK7) substrates for their Kerr-nonlinear refractive indices of 3×10^{-16} cm^2/W and 3.5×10^{-16} cm^2/W, respectively, as well as low absorption. Their dispersion curves [including group delay (GD), group delay dispersion (GDD), and third-order dispersion (TOD)] are shown in Fig. 1(a) for reference.

The general schematic of the cascading is shown in Fig. 1(b). The dispersion compensation after a pass through the material is realized with double-chirped mirrors (DCMs). To find appropriate starting parameters for our experiment, we simulated the pulse broadening in bulk by SPM using the split-step method. The limited number of immediately available optics (DCMs and substrates) restricted the possible combinations and the fine-tuning of the dispersion management. Based on this simulation and this constraint, we chose to design the cascading scheme with three stages of transmission through the substrate and compression as a good compromise between experimental complexity and total nonlinear broadening. These three passes through nonlinear and dispersion-compensating stages mitigate the accumulation of dispersion mismatch.

Figure 1(c) illustrates the simulated behavior of the spectral broadening in FS and BK7 as a function of substrate thickness. The characteristics of the input pulse are close to the experimental ones, with 200 μJ pulse energy and 30 fs compressed initial pulse duration. With three passes in 1.1-mm-thick FS or 0.9-mm-thick BK7 substrates, the spectrum broadens up to 160 nm or 200 nm (foot-to-foot) respectively, with a possible compression down to 10 fs or 8.5 fs.

3. DESCRIPTION OF THE EXPERIMENTAL SETUP

The experimental setup is laid out in Fig. 2(a). A commercial Ti:sapphire laser system based on chirped pulse amplification, delivering nominally 5 mJ, 30-fs-long pulses at a repetition rate of 3 kHz, is used in this experiment. The distance between the two compressor gratings is remotely adjustable. Two beam splitters composed of a half-wave plate (HWP) and a thin-film polarizer (TFP) are used first to split the beam between different experiments, and second to attenuate the energy at the entrance of the pulse compression setup; both TFPs reflect the beam, avoiding the additional dispersion through the FS substrates. The energy in the compression setup is limited to 300 μJ. The beam size is reduced from ∼7 × 6 mm^2 to ∼1.5 mm diameter with two successive telescopes in reflection, minimizing thus the distortions of the spatial profile.

The beam passes three times through a 1-mm-thick, uncoated BK7 or a 2-mm-thick, uncoated FS plate, and is reflected after each pass off DCMs (model UMC10-15FS from Thorlabs) for dispersion compensation. These DCMs are designed to compensate 1.5 mm of FS (54 fs^2) within one bounce. The fine-tuning of the remaining dispersion was realized with supplementary DCMs available in the lab, designed by pair as published by Birge *et al*. [10], compensating nominally ∼52 fs^2 per pair. These DCMs offer a discrete variation in the dispersion management. The incidence angles on the DCMs are minimized. Adjusting slightly the distance between the

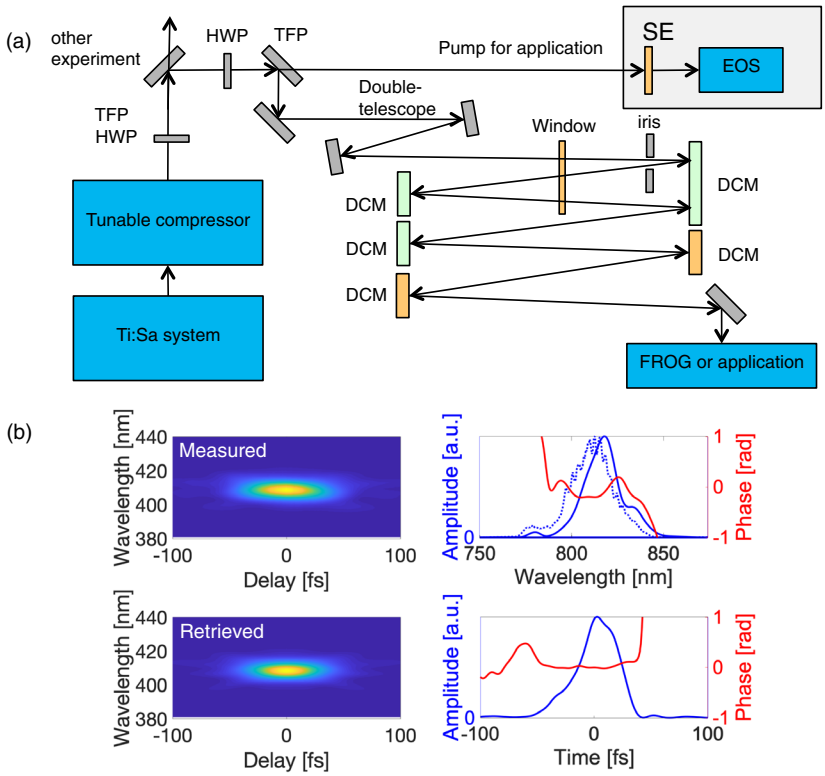

Fig. 2. (a) Layout of the experimental setup. HWP, half-wave plate; TFP, thin-film polarizer; DCM, double-chirped mirror (green, Thorlabs; orange, from [10]); SE, spin emitter sample; EOS, electro-optical sampling. The shaded area corresponds to an application example probed by the shortened pulses. The amount of three DCMs after cascading corresponds to the configuration with the BK7 substrate. Instead, four DCMs after cascading are needed in the case of FS. (b) Pulse characterization with FROG, acquired at the entrance of the pulse compression setup during the second measurement run. Measurement, dotted line; retrieved, plain line.

gratings of the compressor allowed a fine-tuning of the spectral chirp, and a precompensation of the material dispersion. The spatial beam profile exhibits some distortions due to the onset of spatial breakdown (for BK7: $P_{\mathrm{crit}} = 1.79$ MW versus $P_{\mathrm{peak}} = 3.3$ GW). An iris has been added to the setup after the first pass through the substrate to control the beam quality. This suppresses the experimentally observed onset of multiple filaments and increases the daily reliability. The beam goes twice through the iris, with a small angle.

The pulses have been characterized spectrally with an optical spectrometer (OceanOptics HR4000). The electric field and the phases have been retrieved from frequency-resolved optical gating (FROG) measurements. All FROG results are given with the measured and retrieved FROG traces, the measured and retrieved spectral intensities, the retrieved temporal intensity and the spectral and temporal phases. The remaining uncompensated phases are stated at the 5% spectral intensity level.

During our experiments using the compressed pulses, the laser had to be realigned, with slightly changed output pulse characteristics; especially, the higher dispersion orders of the stretcher were not fully matched by the compressor, leading to a remaining uncompensated spectral phase. This modified the compressed pulse with the setup optimized as during the first run. We did two measurement and optimization runs, in which the laser pulse parameters differed both at the laser output and at the entrance of the experimental setup. In the first run, the spectral width amounted to 27 nm (FWHM) and the duration was minimized to 44 fs (FWHM) at the entrance of the pulse compression setup after the optimization of the laser compressor, partly compensating for the dispersion introduced by the half-wave plates; for reference, the minimum pulse duration achievable at the laser output, close to Fourier transform limit, was 38 fs. In the second run, the pulses were compressed to 35 fs at the output of the laser, close to the laser specifications, and reached 71 fs at the entrance of the setup due to the dispersion induced by the two half-wave plates; changing the distance between the gratings of the compressor by 0.13 mm permitted us to shorten the pulses down to 39 fs at the entrance of the setup, as shown in Fig. 2(b). This means that the pulses are not entering the pulse compression setup being transform-limited, and that during the optimization of the pulse compression, it is important to vary the compression position, as a way of balancing the second and higher dispersion orders together.

In the first run of experiments, the best pulse compression results were obtained with a BK7 substrate as broadening medium; the compressor position was shifted by 0.1 mm, leading to a laser pulse duration increase to 54 fs (FWHM) with |3.5 rad| uncompressed phase (or a curvature of $|255\ \mathrm{fs}^2|$ fitting with a parabolic spectral phase) at the input of the compression setup. In the second run of experiments, the 2-mm-long FS substrate with the compressor at the nominal position for a

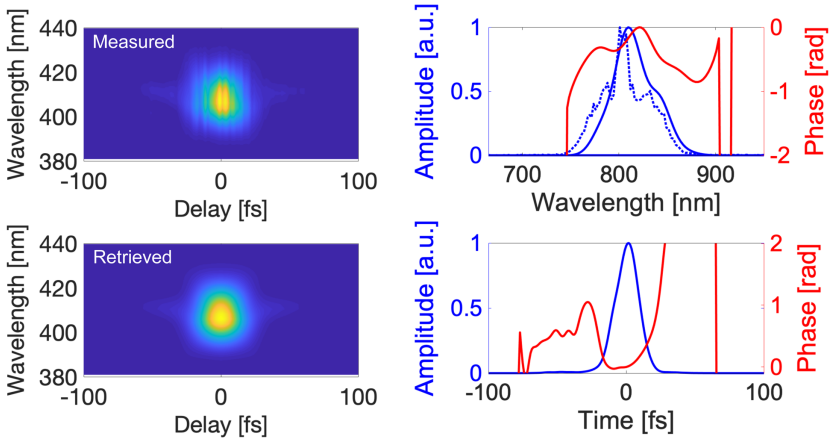

Fig. 3. Typical measurement of daily results with the BK7 substrate. Spectrum: measurement, dotted line; retrieved, plain line.

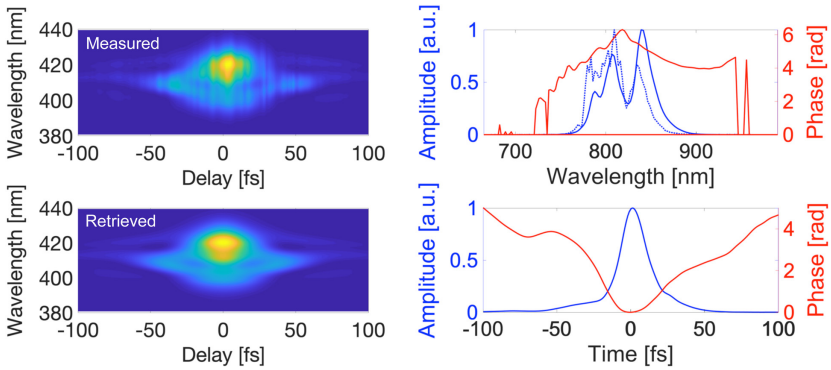

Fig. 4. Typical measurement of daily results with the FS substrate. Spectrum: measurement, dotted line; retrieved, plain line.

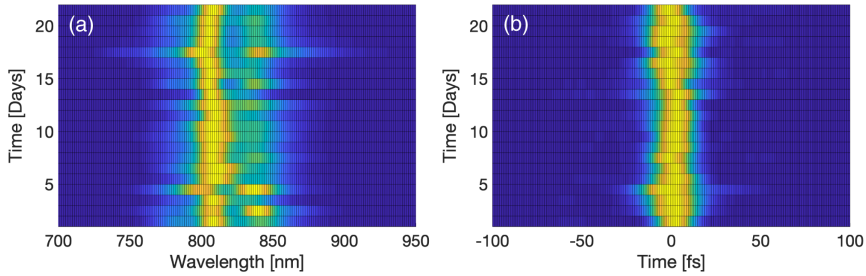

Fig. 5. Day-to-day reproducibility of the (a) spectral and (b) temporal intensity of the pulses.

compressed laser output led to the best results. The calculation of the accumulated dispersion of material and DCMs exhibits a relatively flat profile between 780 nm and 820 nm. Adding three or five more DCMs has been found as optimal dispersion management with the BK7 or FS plate, respectively. Furthermore, in the first run, we optimized the pulse compression setup in two different ways. In the first one, we looked at the shortest achievable pulse duration with this method, pushing the experiment at its limit, which is discussed later in Section 5. For our application, however, day-to-day reproducibility and some margin in the parameter space are required; hence, we optimized for reproducibility at the expense of a slightly longer pulse duration. The second run was only optimized for daily reproducibility. The experimental results of both runs are presented in Figs. 3–5.

4. DAY-TO-DAY RESULTS

The typical results in daily operation are shown in Fig. 3 with the BK7 plate and Fig. 4 with the FS substrate. In both configurations, 200 μJ are used. In the configuration with BK7, the compressor is slightly detuned, so that the entrance pulses are stretched to 54 fs at the entrance of the setup. Three additional DCMs were then needed after the cascading to compress the pulses. The spectrum is broadened in the BK7 substrate to 54 nm (FWHM) and the pulses shortened to 20 fs (FWHM). The remaining parabolic phase amounts to |0.7| rad (or |4| fs^2 curvature).

In the second configuration, with results shown in Fig. 4, the compressor is kept aligned for the shortest possible laser output pulses. After the cascading, four more DCMs have been needed to best compress the spectrally broadened pulses: in

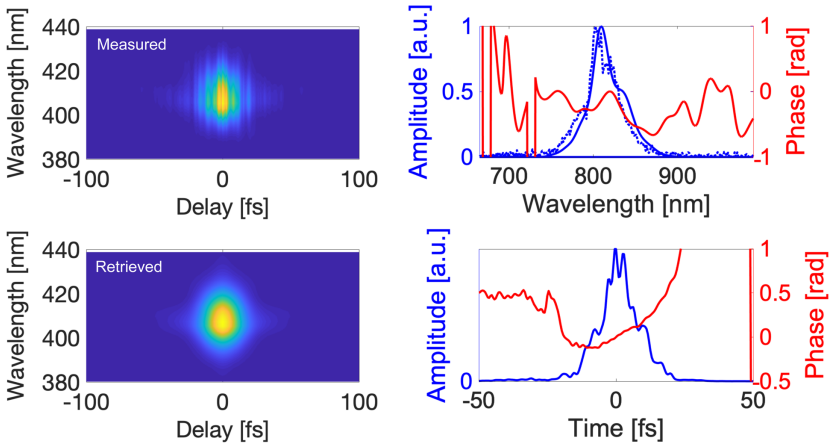

Fig. 6. Shortest pulse duration measured, with 305 μJ input energy. Spectrum: measurement, dotted line; retrieved, plain line.

total there are now five DCMs compensating 1.5 mm of FS, and two DCMs from [10]. The spectrum is broadened to 53 nm (FWHM) and the pulses shortened to 21 fs, with 10 fs^2 uncompensated remaining parabolic phase. This duration is close to the 19 fs transform-limited value.

To demonstrate the day-to-day reproducibility of the pulse parameters, we acquired over several days the FROG data of the uncompressed and compressed pulses, and reconstructed them. This measurement with the BK7 substrate is shown in Fig. 5. Although the spectrum exhibited a repeatable shape, it happened that the shoulder at 840 nm grew more than the main peak at 800 nm even though the pulse duration was typically ∼20 fs.

5. SHORTEST ACHIEVABLE PULSES

The spectral broadening can be extended by increasing the energy of the incoming pulses. When we increased the energy up to 305 μJ, we were able to compress the pulses down to 11 fs, with a remaining uncompensated phase of |0.55| rad (or |3| fs^2 curvature), as shown in Fig. 6. This result was, however, not stable over time, and too much depends on the alignment of the laser compressor and consequently on the fine-tuning of the dispersion management to be obtainable daily. Also the noise of the surroundings of the experiment might have an influence on the stability: vibrations induced by vacuum pumps, long and uncovered optical paths, and stress of the breadboard where the setup is mounted.

6. APPLICATION

We apply these compressed pulses to EOS [11] of THz single-cycle pulses emitted by spin emitters (SEs) [12]; see Fig. 2(a). The part of the (uncompressed) beam labeled as "pump for application" hits a SE sample, which is a stack of non-magnetic and magnetic thin films. The pump leads to local heating within the stack, generating a spin current from the ferromagnetic layer into the external non-magnetic layers, where it is transformed into a charge current via the inverse Spin Hall effect. This charge current radiates in the THz range. An external magnetic field aligns the magnetic domains of the ferromagnetic layer. The

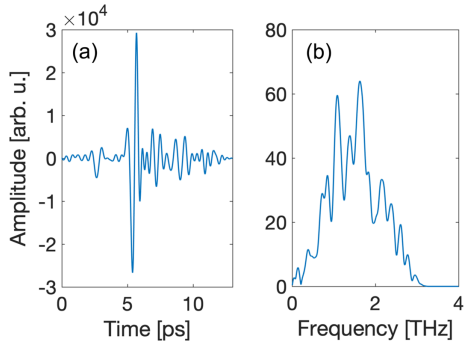

Fig. 7. Electro-optical sampling of a single-cycle THz pulse centered at 1.4 THz, extending up to 4 THz and generated with a spin emitter pumped by the uncompressed part of the Ti:sapphire pulses.

sample used here consists of a Pt (2.1 nm)/Py (1.8 nm)/W (2.0 nm) layer stack on a 0.65-mm-thick sapphire substrate [13]. The EOS detection crystal is a 200-μm-thick ZnTe crystal.

The EOS trace displayed in Fig. 7 shows a single-cycle THz waveform followed by ringing of the EOS crystal. It is deconvoluted to remove different effects (Fabry–Perot interference as well as absorption and dispersion of the THz in the EOS crystal, frequency and orientation dependences of the latter, resolution of the probe and pump–probe overlap) [14,15]. The resulting spectrum extends up to 3 THz (foot-to-foot) and is centered at 1.4 THz. These frequencies correspond to 330 fs and 710 fs, respectively.

7. CONCLUSION

We present a compact, easy-to-align pulse compression scheme in bulk material. We demonstrated a robust shortening of the pulse duration by a factor of 2.5 on a daily basis, and even ∼5 with fully matched dispersion compensation. As an example application, we use the compressed pulses for EOS of a single-cycle THz waveform from a thin-film SE, centered at 1.4 THz and extending up to 3 THz.

Funding. Helmholtz-Fonds (PD-303).

Disclosures. The authors declare no conflicts of interest.

REFERENCES

1. R. R. Alfano and S. L. Shapiro, "Observation of self-phase modulation and small-scale filaments in crystals and glasses observation of self-phase modulation and small-scale filaments in crystals and glasses," Phys. Rev. Lett. **24**, 592–594 (1970).
2. N. Bloembergen, "The influence of electron plasma formation on superbroadening in light filaments," Opt. Commun.**8**, 285–288 (1973).
3. P. Balla, A. Bin Wahid, I. Sytcevich, C. Guo, A.-L. Viotti, L. Silletti, A. Cartella, S. Alisauskas, H. Tavakol, U. Grosse-Wortmann, A. Schönberg, M. Seidel, A. Trabattoni, B. Manschwetus, T. Lang, F. Calegari, A. Couairon, A. L'Huillier, C. L. Arnold, I. Hartl, and C. M. Heyl, "Postcompression of picosecond pulses into the few-cycle regime," Opt. Lett. **45**, 2572–2575 (2020).
4. A. Kessel, S. A. Trushin, N. Karpowicz, C. Skorbol, S. Klingebiel, C. Wandt, and S. Karsch, "Generation of multi-octave spanning high-energy pulses by cascaded nonlinear processes in BBO," Opt. Express**24**, 5628–5637 (2016).
5. J. E. Beetar, S. Golam-Mirzaei, and M. Chini, "Spectral broadening and pulse compression of a 400 μJ, 20 W Yb:KGW laser using a multi-plate medium," Appl. Phys. Lett.**112**, 051102 (2018).
6. M. Nisoli, S. De Silvestri, and O. Svelto, "Generation of high energy 10 fs pulses by a new pulse compression technique," Appl. Phys. Lett. **68**, 2793–2795 (1996).
7. B.-H. Chen, M. Kretschmar, D. Ehberger, A. Blumenstein, P. Simon, P. Baum, and T. Nagy, "Compression of picosecond pulses from a thin-disk laser to 30 fs at 4 W average power," Opt. Express**26**, 3861–3869 (2018).
8. S. Hädrich, M. Kienel, M. Müller, A. Klenke, J. Rothhardt, R. Klas, T. Gottschall, T. Eidam, A. Drozdy, P. Jójárt, Z. Várallyay, E. Cormier, K. Osvay, A. Tünnermann, and J. Limpert, "Energetic sub-2-cycle laser with 216 W average power," Opt. Lett. **41**, 4332–4335 (2016).
9. M. Bache, H. Guo, and B. Zhou, "Generating mid-IR octave-spanning supercontinua and few-cycle pulses with solitons in phase-mismatched quadratic nonlinear crystals," Opt. Mater. Express **3**, 1647–1657 (2013).
10. J. R. Birge and F. X. Kärtner, "Efficient optimization of multilayer coatings for ultrafast optics using analytic gradients of dispersion," Appl. Opt.**46**, 2656–2662 (2007).
11. A. Leitenstorfer, S. Hunsche, J. Shah, M. C. Nuss, and W. H. Knox, "Detectors and sources for ultrabroadband electro-optic sampling: experiment and theory," Appl. Phys. Lett.**74**, 1516–1518 (1999).
12. T. Seifert, S. Jaiswal, U. Martens, J. Hannegan, L. Braun, P. Maldonado, F. Freimuth, A. Kronenberg, J. Henrizi, I. Radu, E. Beaurepaire, Y. Mokrousov, P. M. Oppeneer, M. Jourdan, G. Jakob, D. Turchinovich, L. M. Hayden, M. Wolf, M. Münzenberg, M. Kläui, and T. Kampfrath, "Efficient metallic spintronic emitters of ultrabroadband terahertz radiation," Nat. Photonics **10**, 483–488 (2016).
13. E. Kueny, A.-L. Calendron, S. Velten, L. Bocklage, F. X. Kärtner, and R. Röhlsberger, (to be published).
14. E. Kueny, A.-L. Calendron, and F. X. Kärtner, "Electro-optic sampling of terahertz pulses in multilayer crystals," in *Laser Congress (ASSL, LAC, LS&C)* (2019), paper JTu3A.16.
15. J. Faure, J. Van Tilborg, R. A. Kaindl, and W. P. Leemans, "Modelling laser-based table-top THz sources: optical rectification, propagation and electro-optic sampling," Opt. Quantum Electron. **36**, 681–697 (2004).